AD-A141 315 INVESTIGATION OF ACOUSTIC EMISSION DURING FRACTURE TOUGHNESS TESTING OF C.. (U) NAVAL WEAPONS CENTER CHINA LAKE CA J L STOKES ET AL. MAR 84 NWC-TP-6476 1/1

UNCLASSIFIED SBI-AD-E900 338 F/G 11/6 NL

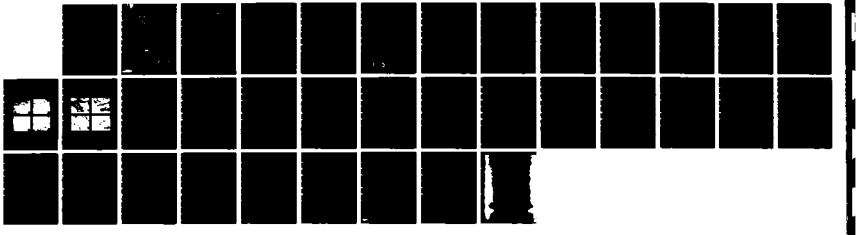

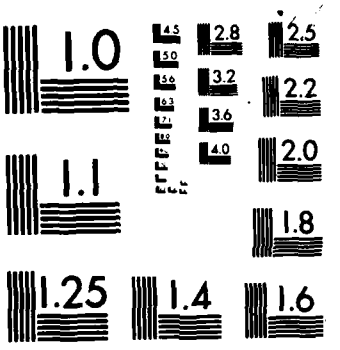

NWC TP 6476

(12)

Investigation of Acoustic Emission During Fracture Toughness Testing of Chevron-Notched Specimens

by
J. L. Stokes
and
G. A. Hayes
Engineering Department

MARCH 1984

NAVAL WEAPONS CENTER
CHINA LAKE, CALIFORNIA 93555

Naval Weapons Center
AN ACTIVITY OF THE NAVAL MATERIAL COMMAND

FOREWORD

A study investigating the relationship between fracture toughness of engineering materials and acoustic emission phenomena was authorized by the Naval Air Systems Command under Task Assignment Number A420401/008-6/3420000003. The experimental work was performed during FY 1983. The purpose of the study was to determine the correlation between acoustic emission during stress application and the fracture toughness of four different ferrous alloys. This report is the first of a series investigating the factors influencing acoustic emission from stressed structural materials used in missile applications.

This report has been reviewed for technical accuracy by professional reviewers provided by the American Society for Testing and Materials (ASTM).

Approved by
D. J. RUSSELL, *Head*
Engineering Department
10 February 1984

Under Authority of
K. A. DICKERSON
Capt., U.S. Navy
Commander

Released for publication by
B. W. HAYS
Technical Director

NWC Technical Publication 6476

Published by ..... Engineering Department
Collation ..... Cover, 16 leaves
First printing ..... 150 unnumbered copies

UNCLASSIFIED

SECURITY CLASSIFICATION OF THIS PAGE *(When Date Entered)*

REPORT DOCUMENTATION PAGE

READ INSTRUCTIONS BEFORE COMPLETING FORM

1. REPORT NUMBER: NWC TP 6476	2. GOVT ACCESSION NO.: AD-A141 315
3. RECIPIENT'S CATALOG NUMBER:	
4. TITLE *(and Subtitle)*: INVESTIGATION OF ACOUSTIC EMISSION DURING FRACTURE TOUGHNESS TESTING OF CHEVRON-NOTCHED SPECIMENS	5. TYPE OF REPORT & PERIOD COVERED: Final Report 1982-1983
	6. PERFORMING ORG. REPORT NUMBER:
7. AUTHOR(s): J. L. Stokes and G. A. Hayes	8. CONTRACT OR GRANT NUMBER(s):
9. PERFORMING ORGANIZATION NAME AND ADDRESS: Naval Weapons Center, China Lake, CA 93555	10. PROGRAM ELEMENT, PROJECT, TASK AREA & WORK UNIT NUMBERS: Air Task No. A420401/008-6/ 3420000003 of 1 October 1982
11. CONTROLLING OFFICE NAME AND ADDRESS: Naval Weapons Center, China Lake, CA 93555	12. REPORT DATE: March 1984
	13. NUMBER OF PAGES: 29
14. MONITORING AGENCY NAME & ADDRESS *(if different from Controlling Office)*:	15. SECURITY CLASS. *(of this report)*: UNCLASSIFIED
	15a. DECLASSIFICATION/DOWNGRADING SCHEDULE:

16. DISTRIBUTION STATEMENT *(of this Report)*

Approved for public release; distribution unlimited.

17. DISTRIBUTION STATEMENT *(of the abstract entered in Block 20, if different from Report)*

18. SUPPLEMENTARY NOTES

19. KEY WORDS *(Continue on reverse side if necessary and identify by block number)*

acoustics	emission
fracture (materials)	fracture toughness tests
toughness	cracking (fracturing)
steels	steel castings

20. ABSTRACT *(Continue on reverse side if necessary and identify by block number)*

See back of form.

DD FORM 1 JAN 73 1473 EDITION OF 1 NOV 65 IS OBSOLETE

S/N 0102-LF-014-6601

UNCLASSIFIED

SECURITY CLASSIFICATION OF THIS PAGE *(When Date Entered)*

(U) *Investigation of Acoustic Emission During Fracture Toughness Testing of Chevron-Notched Specimens*, by J. L. Stokes and G. A. Hayes. Naval Weapons Center, March 1984. 29 pp. (NWC TP 6476, publication UNCLASSIFIED.)

(U) Acoustic Emission (AE) monitoring in conjunction with fracture toughness testing of chevron-notched specimens was employed to investigate crack growth in four steels prepared by electroslag-remelt casting. 15-5PH, AISI 4140, D6AC, and AISI 440C were investigated. AE data were recorded and correlated with variations in fracture toughness test behavior and fracture surface topography. AE parameters such as total counts, count rate, amplitude distribution, etc., were used to characterize flow and fracture processes. AE measurements were observed to have good correlation with crack growth parameters and the energetics of discrete cracking events.

CONTENTS

Introduction 3

Experimental Procedures. 3
Materials 3
Fracture Toughness Testing. 4
Acoustic Emission Monitoring. 4

Results and Discussion 5
Load Versus Displacement. 5
Load Versus Acoustic Emission Counts. 5
Acoustic Emission Count Rate Versus Time
(Load Versus Time Superimposed) 6
Log-Sum Amplitude Distributions 6
Noise 7

Summary. 7

Conclusions. 8

ACKNOWLEDGMENT

This report is based on part of the results of a study of ESR casting technology sponsored by the U. S. Naval Air Systems Command, Washington, D.C.

The authors wish to express their thanks to C. A. Johnson for providing the ESR ingots for fracture toughness and acoustic emission evaluation.

INTRODUCTION

In recent years there has been considerable interest in the development of a standardized fracture toughness test utilizing chevron-notched specimens.[1-4] These investigations have determined that crack growth behavior in chevron-notched specimens depend in part on the microstructural characteristics of a material, as well as inherent material properties, i.e., yield strength, fracture toughness, work hardening rate, etc. For example, depending on the material, heat treatment or test environment, crack growth can occur continuously with applied load, or in a discontinuous mode (crack jumps), with varying amounts of plastic yielding occurring at the crack tip. The fracture mode can range from fibrous failure to cleavage cracking.

Recent advances in acoustic emission (AE) technology have shown that AE activity in a metal, regardless of the method of mechanical testing, depends upon metallurgical variables such as composition, and heat treatment.[5] The purpose of this investigation was to determine the feasibility of using AE for monitoring the initiation and propagation of cracks in chevron-notched specimens in order to characterize cracking mechanisms.

EXPERIMENTAL PROCEDURES

Materials

Four different cast steel compositions were tested in this investigation: 15-5PH, AISI 4140, D6AC and AISI 440C. The composition of each steel is given in Table 1. Castings were prepared by electroslag remelting (ESR) the alloys into ingots approximately 200mm (8-inches) long by 76mm (3-inches) in diameter. Each steel was heat

---

[1] Barker, L. M., Engineering Fracture Mechanics, Vol. 9, 1977, p. 361.

[2] Barker, L. M. and Leslie, W. C., in Fracture 1977, Vol. 2, 4th International Conference on Fracture, Waterloo, Canada, 1977, p. 305.

[3] Barker, L. M., "Short Bar Specimens for K_{Ic} Measurements", Fracture Mechanics Applied to Brittle Materials, ASTM STP 678, S. W. Frieman, Ed., American Society for Testing and Materials, 1979, pp. 73-82.

[4] Barker, L. M., "Short Rod and Short Bar Fracture Toughness Specimen and Geometrics and Test Methods for Metallic Materials", Fracture Mechanics: Thirteenth Conference, ASTM STP 743, Richard Roberts, Ed, American Society for Testing and Materials, 1981, pp. 456-475.

[5] Wadley, H. N. G., Scruby, C. B. and Speake, J. H., International Metallurgical Reviews, Vol. 2, 1980, p. 41.

treated to a common commercially-used condition, then characterized by measuring hardness, yield and ultimate strengths and percent elongation. The heat treatment given each steel and the resulting mechanical properties are presented in Table 2. (No tensile data are shown for AISI 440C. The specimens were so brittle that they shattered in the grips.) The microstructure of each alloy is shown in Figure 1. Figures 1a, 1b, and 1c show uniform matrices of tempered martensite typical of the respective alloy and heat treatment. Figure 1d (AISI 440C) shows a tempered martensite matrix containing large primary carbides at the grain boundaries, also typical of this alloy in the cast condition.

Fracture Toughness Testing

Chevron-notched fracture toughness specimens (25.4mm (1-inch) in diameter) were machined from the cast ESR ingots. Test specimen configuration and dimensions are described elsewhere.[1] The specimens were heat treated before the thin longitudinal chevron slots were cut. The chevron-notched rods were tested at ambient temperature in air using a TerraTek screw-driven mechanical test machine.[2] Fracture toughness values were determined using the method developed by Barker.[3] All fracture surfaces were characterized by means of the scanning electron microscope (SEM). An SEM fractograph of each material is shown in Figure 2. These are interesting in that they all indicate brittle fracture modes. This is especially apparent in Figure 2a (15-5PH) which shows cleavage exclusively. Although somewhat less well defined, it appears that the AISI 4140 (Figure 2b) and the D6AC (Figure 2c) failed primarily by cleavage also. The fracture illustrated in Figure 2d (AISI 440C) is unique in that it shows cleavage of the second-phase carbides, and evidence of intergranular fracture of the matrix.

Acoustic Emission Monitoring

Fracture toughness tests of each steel were acoustically monitored using commercially available Dunegan/Endevco (DE) 3000 series instrumentation. The acoustic pick-up was a 100 kHz resonant piezoelectric transducer (Model DE S9204). The signals from the transducer were processed in a signal conditioning unit incorporating a DE 302A amplifier with gain of 50dB; a DE 1801 preamplifier with gain of 40dB; band pass filters between 100 kHz and 2 MHz to remove extraneous noise; a DE 920A distribution analyzer and DE 921 amplitude detector to sum the number of acoustic emissions greater than a pre-selected threshold of 30dB. AE data was recorded with a Hewlett-Packard (HP) 9825B computer for subsequent playback and analysis.

Because of the geometry of the TerraTek loading fixture, it was necessary to use a spacer between the test specimen and the transducer. The spacer was a 25.4mm (1-inch) diameter by 12.7mm (0.5-inch) cylinder of PH13-8Mo, Condition H1125, corrosion resistant steel. The test specimen, spacer and transducer were coupled with DE water-soluble acoustic couplant.

RESULTS AND DISCUSSION

Load Versus Displacement

Figure 3 shows parametric plots of load versus displacement for each alloy. In each case, the specimen was slowly loaded until a crack was intitiated. A continously increasing load was required to advance the crack until it reached a critical length, where the load went through a maximum. Two or more relaxation and reloading cycles were made when the load was near the maximum value to allow calculation of the degree to which linear elastic fracture mechanics conditions had been violated.[3]

For the 15-5PH, D6AC and AISI 440C, the second unloading represented the end of the test. In the case of the AISI 4140, a third load/unload sequence was made in order to calculate the fracture toughness associated with each substantial crack jump. In the crack jump case, the fracture toughness was taken at the average of several values of fracture toughness calculated after each major crack jump.

The fracture toughness values computed for each alloy are shown in Table 3. The data show that fracture toughness was inversely proportional to strength and hardness. Thus, the AISI 440C at a hardness of HRC 57 exhibited a fracture toughness of 40.2MPa$\sqrt{m}$ (37ksi$\sqrt{in}$), and the 15-5PH at a hardness of HRC 43 exhibited a fracture toughness of 79.2MPa$\sqrt{m}$ (72ksi$\sqrt{in}$). As shown in Table 3, the remaining two alloys were intermediate in hardness and toughness.

Load Versus Acoustic Emission Counts

Figure 4 shows plots of relative load versus cumulative acoustic emission (AE) counts. It can be seen from the plots that although the same criterion for unloading was used in each case, the total AE counts generated up to the first unloading point varied significantly from one alloy to the next. Thus, the toughest alloy, 15-5PH, generated approximately 1.5×10^5 counts up to the first unloading; whereas, the most brittle alloy, AISI 440C, generated approximately 6.2×10^5 counts up to the first unloading point.

Acoustic Emission Count Rate Versus Time (Load Versus Time Superimposed)

Figure 5 shows AE count rate versus time. Superimposed on each plot is a plot of load versus time. These plots show that essentially all of the AE was generated during loading. (The AE observed during the final unloading should be ignored. The gross "noise" was generated by the specimen separating rapidly into two halves.)

A comparison of count rates during the first load/unload cycle between the four alloys confirms the trend observed in Figure 4. That is, the toughest alloy had a relatively low count rate, 2.8×10^5 counts/second during the first cycle, and the most brittle alloy had a much higher count rate, 9.6×10^5 counts/second during the first cycle.

Log-Sum Amplitude Distributions

Figure 6 contains log-sum amplitude distributions showing AE cumulative counts on the vertical axis and amplitude in dB on the horizontal axis. In each case, the threshold was set to exclude signals below 30dB. Cumulative amplitude distributions were recorded at 6 second intervals throughout each test.

At least four distributions are shown for each test. The first distribution in each figure shows cumulative AE events versus amplitude up to the first unloading point. Thus, the first distribution represents primarily plastic deformation and crack initiation. The second distribution in each figure is the one immediately following the first. That is, the one recorded 6 seconds later in the test. For Figure 6b only, a third distribution is shown taken 6 seconds after the second distribution. The next to last distribution in each figure was recorded at the second unloading point. And finally, the last distribution in each figure is the cumulative amplitude distribution for the entire test.

The significance of these comparisons is that for all four alloys a distinct change in amplitude distribution was observed after the first unloading point. This point would seem to mark the transition from crack initiation to slow crack growth. From this point on, the amplitude distributions remained essentially the same.

According to Pollack,[6] the shape of the log-sum amplitude distribution can in many cases be related to the fracture toughness of the material. Pollack shows that for most engineering materials the slope, b, will be between 0.7 and 1.5 with occasional values as low as 0.4 or as high as 4.0. He states that the lowest b-values are found for discontinuous crack growth processes in brittle materials, while plastic deformation prior to crack growth gives relatively high b-values.

In each of the figures 6a through 6d, b-values are shown for the first and the last distributions. It will be noted that the final distribution in Figure 6b has two b-values, and the final distribution in Figure 6c has three b-values. It is also interesting to note that in Figures 6b and 6d representing AISI 4140 and AISI 440C respectively, the b-values for the first distribution were identical.

The b-value data are summarized in Table 3. In general, these values are in accordance with Pollack's data showing high values for plastic deformation and low values for slow crack growth. In this case, however, it appears that the higher b-values represent a combination of plastic deformation and microcracking. It is apparent also that for this series of tests the b-values were not proportional to fracture toughness.

Noise

To determine the contribution of noise to the total AE signal, a dummy specimen (without a sharp notch) was instrumented and loaded well into the elastic range several times. The AE response recorded during the final load cycle is shown in Figure 7. Figure 7a shows total AE counts versus time, and Figure 7b shows count rate versus time. These data show that noise constituted approximately 5 percent of the total AE activity monitored during fracture toughness testing.

SUMMARY

When testing chevron-notched specimens, it was found that the AE count rate during loading varied significantly from one alloy to the next depending on fracture toughness. This is reflected in Table 3 by the total AE counts at the first unloading point. A comparison of fracture toughness to total counts at the first unloading point provided a relative measure of fracture toughness, i.e., the lower the fracture toughness the higher the count rate. This can be attributed to microcracking processes initiated early in the first loading cycle. In all cases, AE was observed only on loading.

---

[6] Pollock, A. A., Int. Adv. in Nondestructive Testing, Vol. 7, 1981, pp. 215-239.

Log-sum amplitude distributions were used to characterize initial and final stages of crack growth. For all materials a distinct change in amplitude distribution was observed after the first unloading point. From this point on, the amplitude distributions remained essentially the same throughout the test. It appears, therefore, that in all cases the initial amplitude distribution was characteristic of plastic deformation and crack initiation, and that all subsequent distributions represented crack growth. The slopes (b-values) of the amplitude distributions were measured as suggested by Pollack, and, in general, the b-values were in agreement with Pollack's data.

CONCLUSIONS

The following conclusions can be made in regard to AE monitoring of chevron-notched fracture toughness tests:

(1) AE count and count rate are directly relatable to fracture toughness values; the tougher alloys produced a relatively low total count and count rate while more brittle alloys produced a much higher total count and count rate.

(2) A distinct change in amplitude distribution occurs during the transition from crack initiation to crack growth.

(3) Log-sum amplitude distribution analysis indicates high values of the b parameter during the plastic deformation and crack-initiation stages of testing and low values of b for slow crack growth.

(4) For this series of tests, b-values are not proportional to fracture toughness.

(5) AE measurements provide a possible means for relating fracture toughness to material phenomena (plastic deformation, microcrack formation, crack growth).

TABLE 1. Chemical Analyses Of Materials

Alloy	Element, % by Weight											
	C	Mn	P	S	Si	Cu	Cr	Ni	Mo	Cb	V	Fe
15-5PH	0.04	0.66	0.003	0.004	0.33	3.56	14.95	4.20	-	0.35	-	*
AISI 4140	0.42	0.88	0.004	0.007	0.26	-	1.00	-	0.21	-	-	*
D6AC	0.46	0.74	0.002	0.002	0.29	0.18	1.01	0.59	1.05	-	0.09	*
AISI 440C	1.02	0.50	0.003	0.002	0.22	-	16.50	0.28	0.45	-	-	*

* Remainder

TABLE 2. Mechanical Properties of Fracture Toughness Specimens

Alloy	Heat Treatment	0.2% Offset Yield Strength, MN/m^2 (ksi)	Ultimate Tensile Strength, MN/m^2 (ksi)	% Elongation 25.4mm (1-inch)	Hardness HRC
15-5PH	Condition H900	1172 (170)	1276 (185)	12	43
AISI 4140	857°C (1575°F)-QQ 385°C (725°F) Temper	1441 (209)	1544 (224)	10	47
D6AC	899°C (1650°F)-QQ 427°C (800°F) Temper	1469 (213)	1655 (240)	8	49
AISI 440C	1038°C (1900°F) 191°C (375°F) Temper	Broke in grips (Too brittle)		-	57

TABLE 3. Summary of Test Results

Material	Fracture Toughness MPa√m (ksi√in)	AE Counts at first loading	b-value	
			Initial Distribution	Final Distribution
15-5PH	79.0 (72)	1.5×10^5	1.05	0.29
AISI 4140	69.3 (63)	2.3	0.83	0.87/0.36
D6AC	66.8 (61)	4.8	1.18	0.64/0.18/0.31
AISI 440C	40.2 (37)	6.2	0.83	0.53

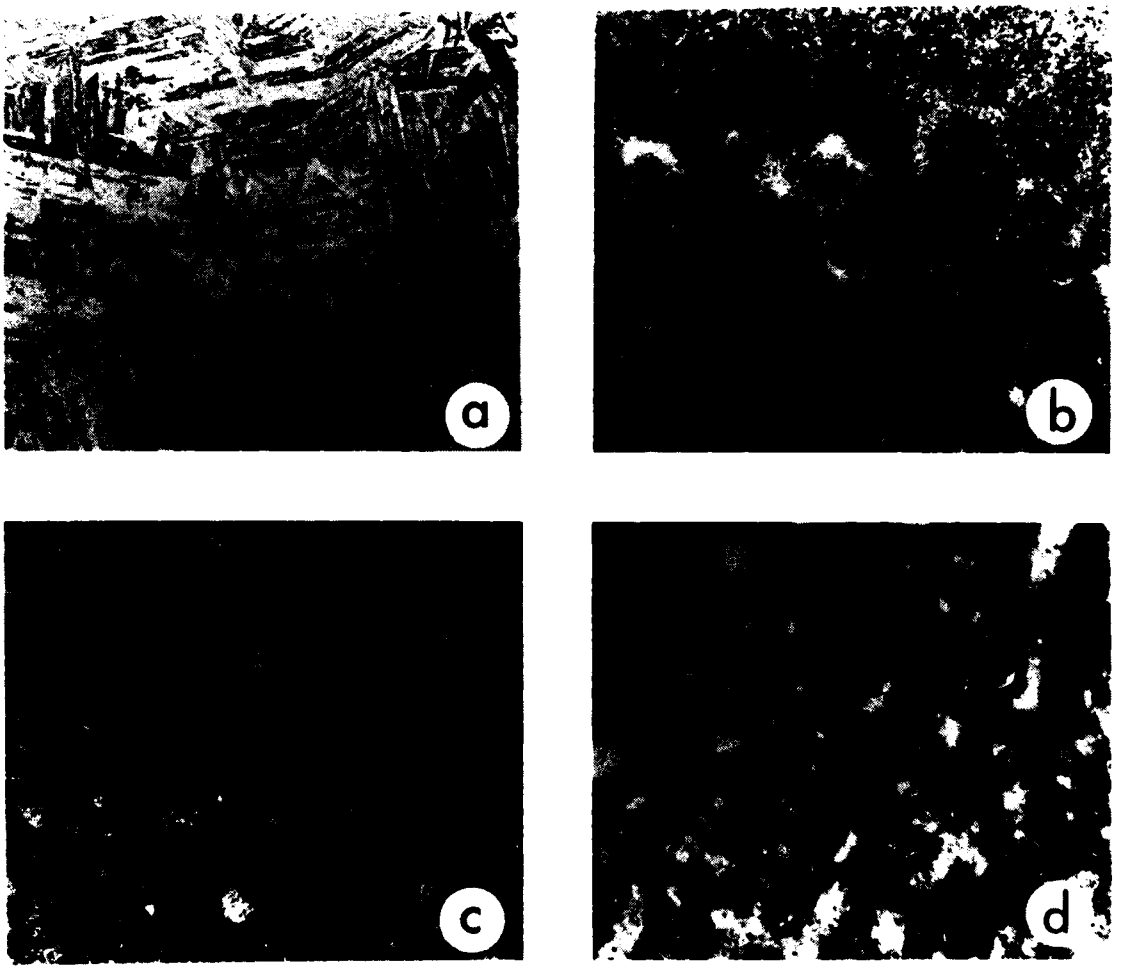

FIGURE 1. Microstructures of chevron-notched fracture toughness specimens with original magnification at 200X. (a) is 15-5PH, (b) is AISI 4140, (c) is D6AC, and (d) is AISI 440C.

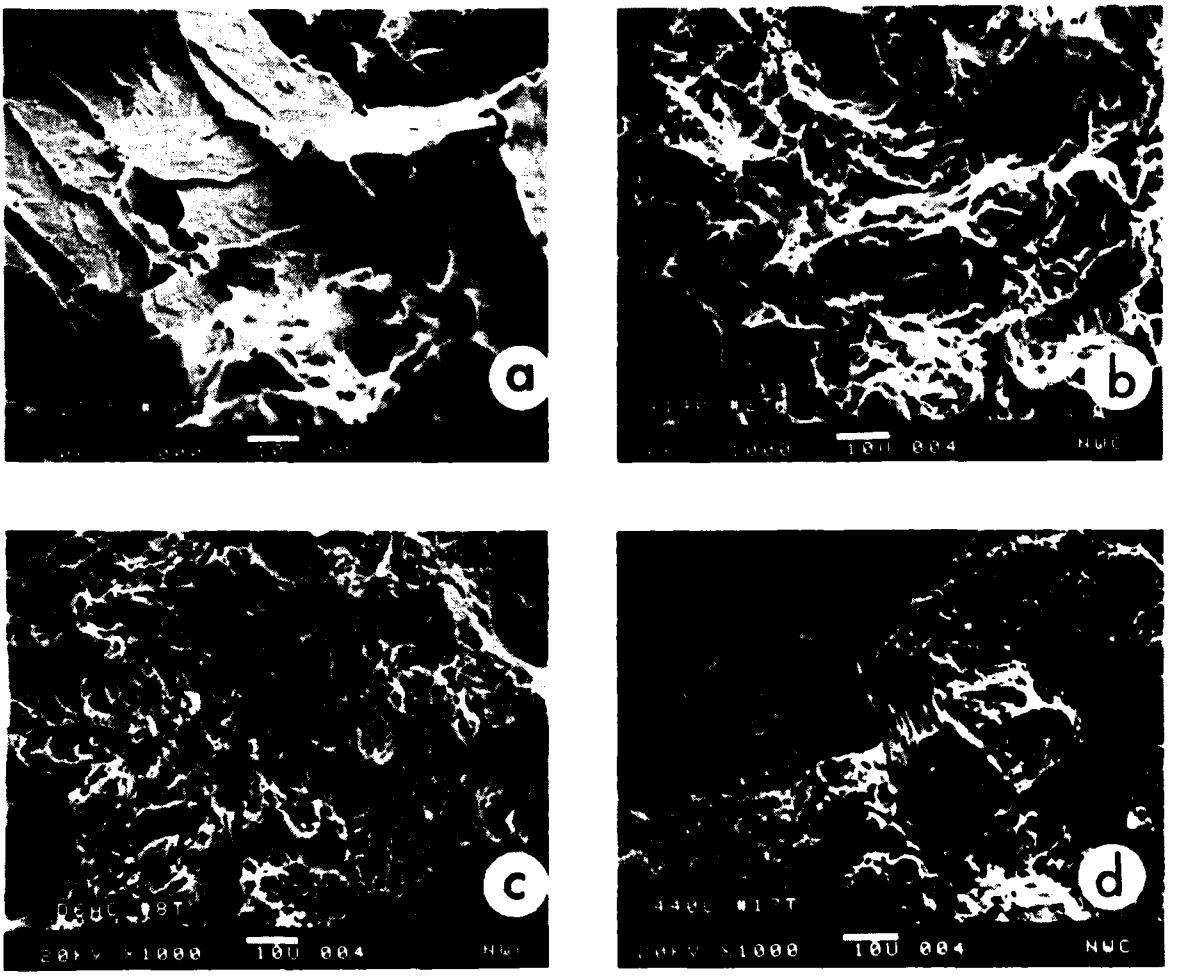

FIGURE 2. SEM fractographs of chevron-notched fracture toughness specimens with original magnification at 1000X. (a) is 15-5PH, (b) is AISI 4140, (c) is D6AC, and (d) is AISI 440C.

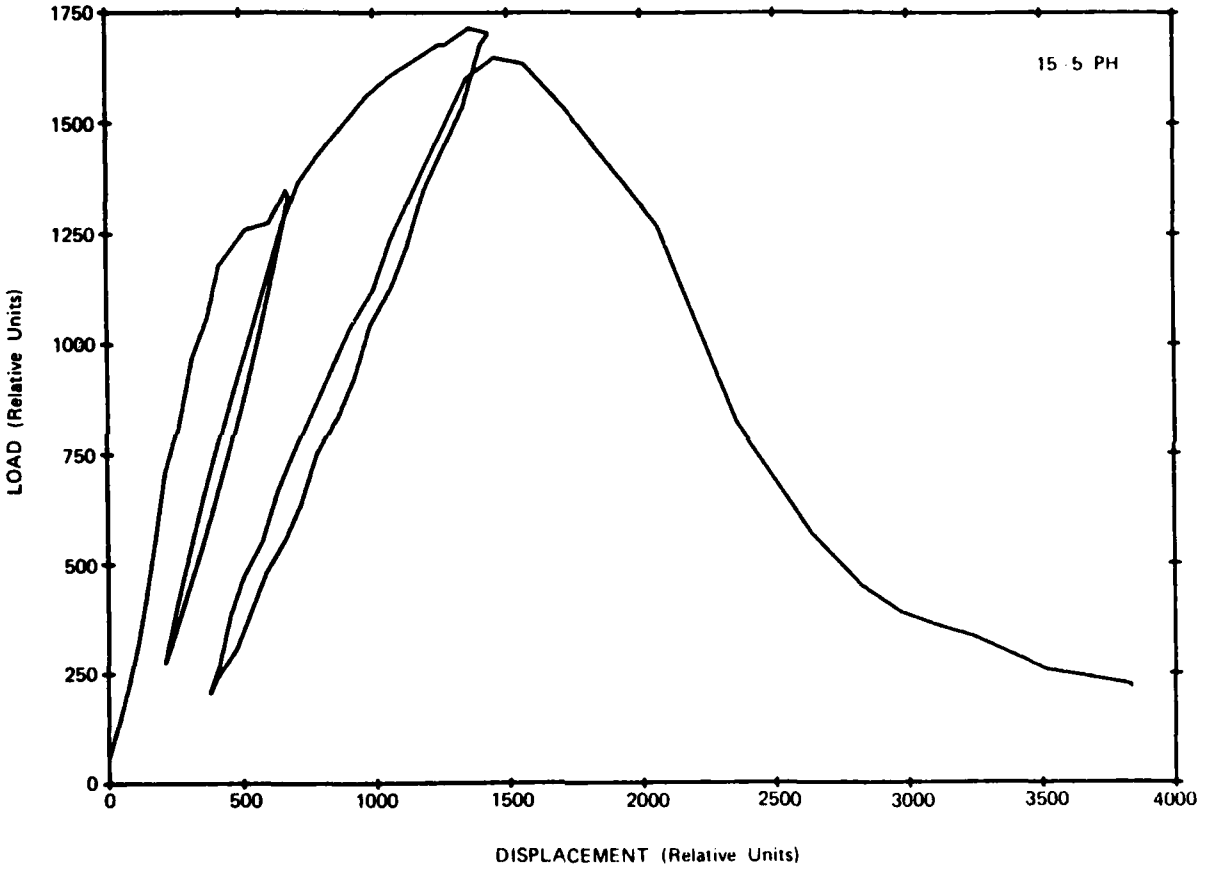

FIGURE 3 (a). Load versus displacement for chevron-notched fracture toughness specimen, 15-5PH.

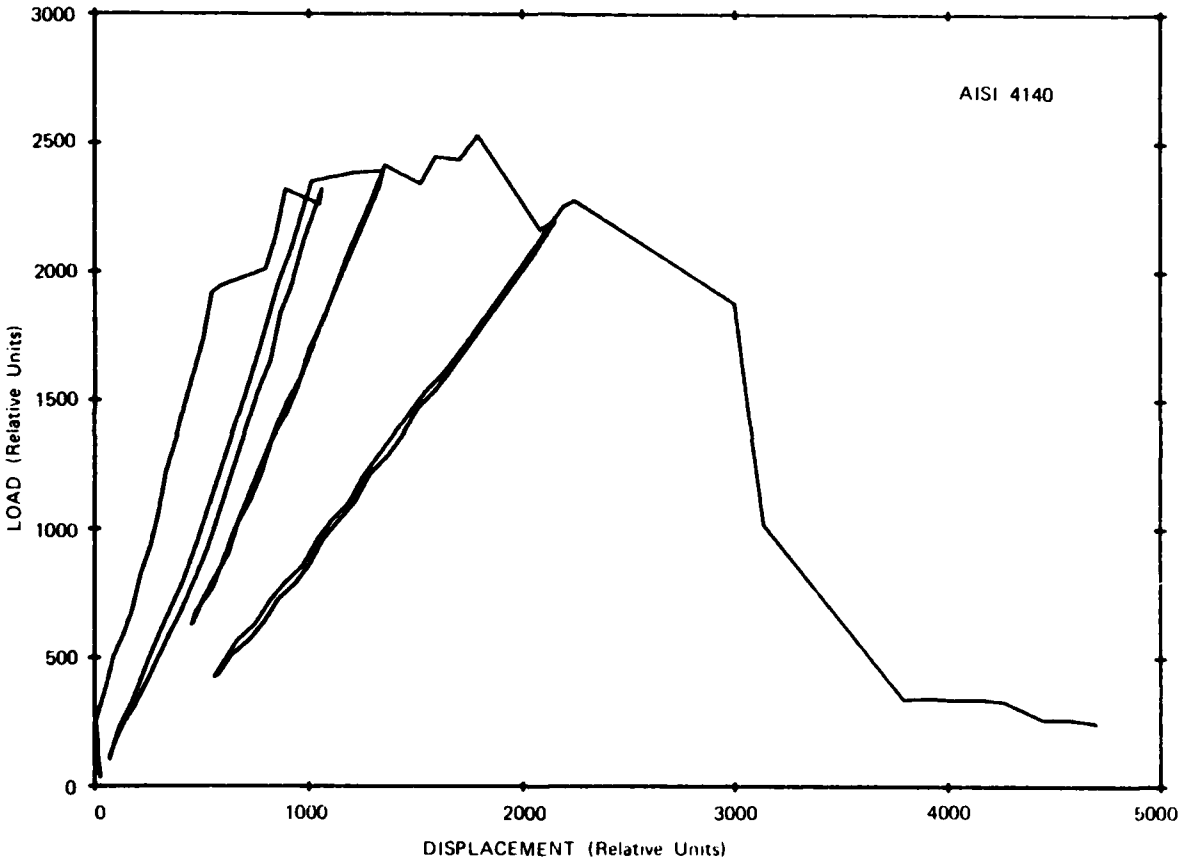

FIGURE 3 (b). Load versus displacement for chevron-notched fracture toughness specimen, AISI 4140.

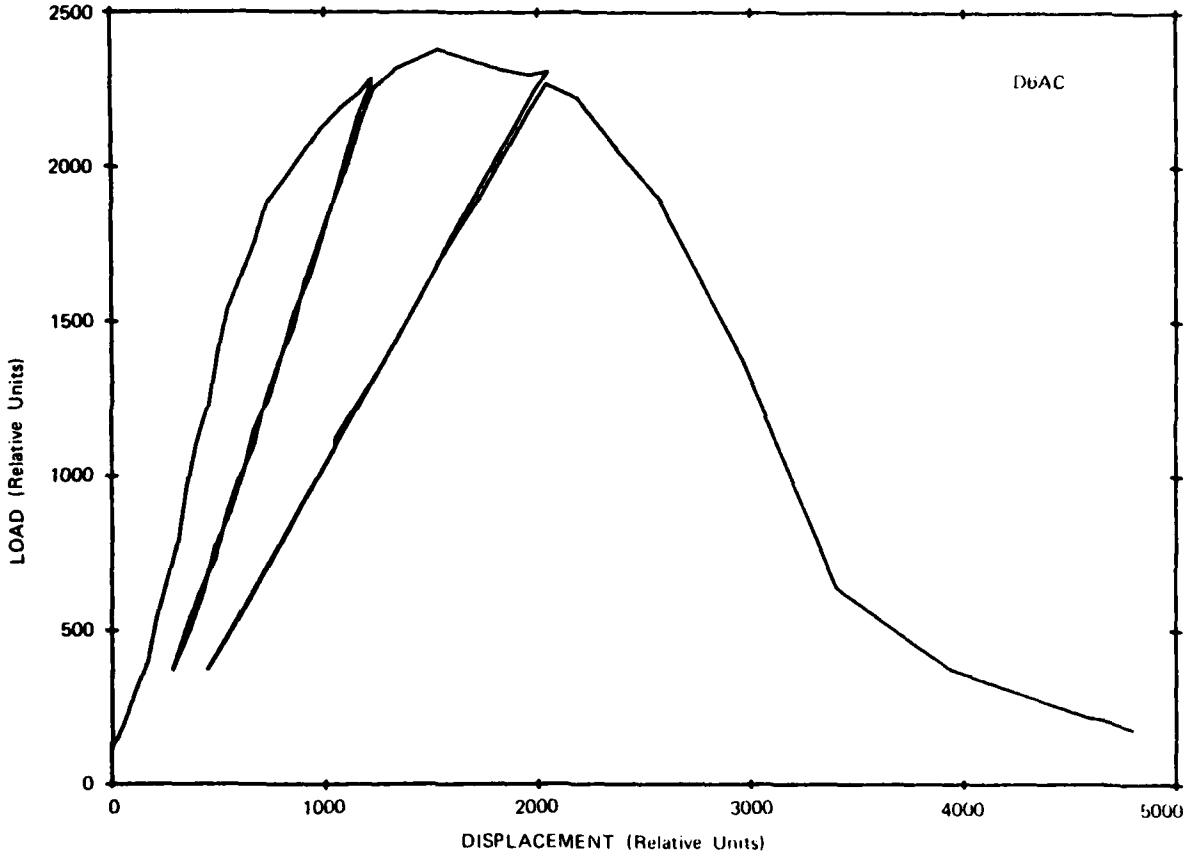

FIGURE 3 (c). Load versus displacement for chevron-notched fracture toughness specimen, D6AC.

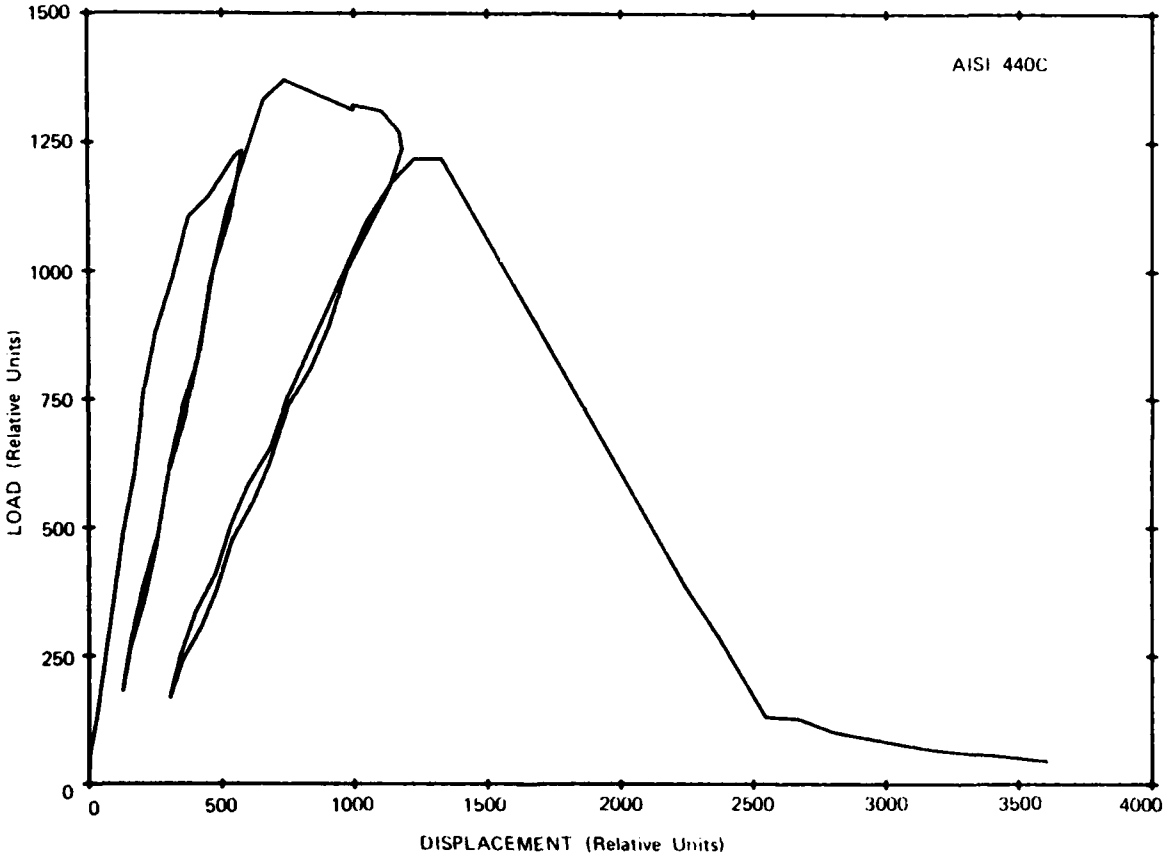

FIGURE 3 (d). Load versus displacement for chevron-notched fracture toughness specimen, AISI 440C.

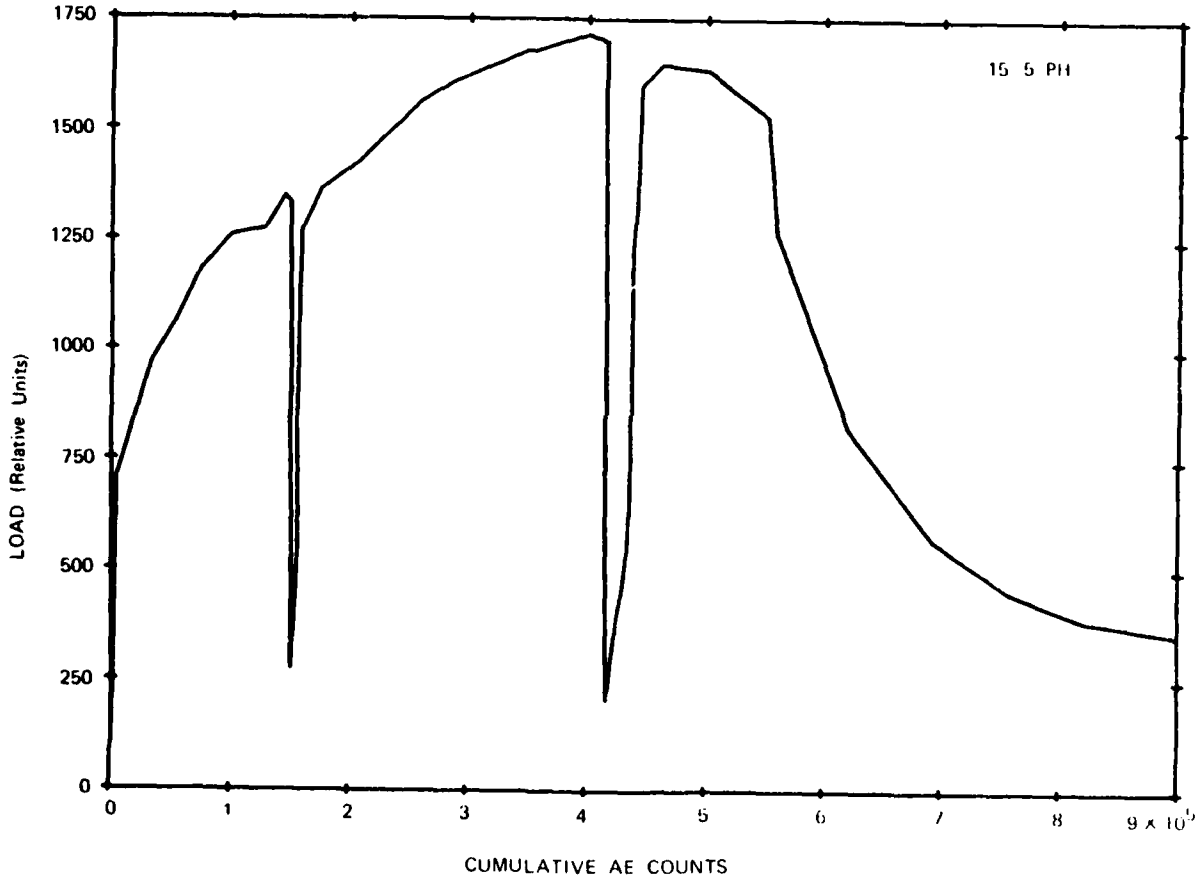

FIGURE 4 (a). Load versus cumulative AE counts for chevron-notched fracture toughness specimen, 15-5PH.

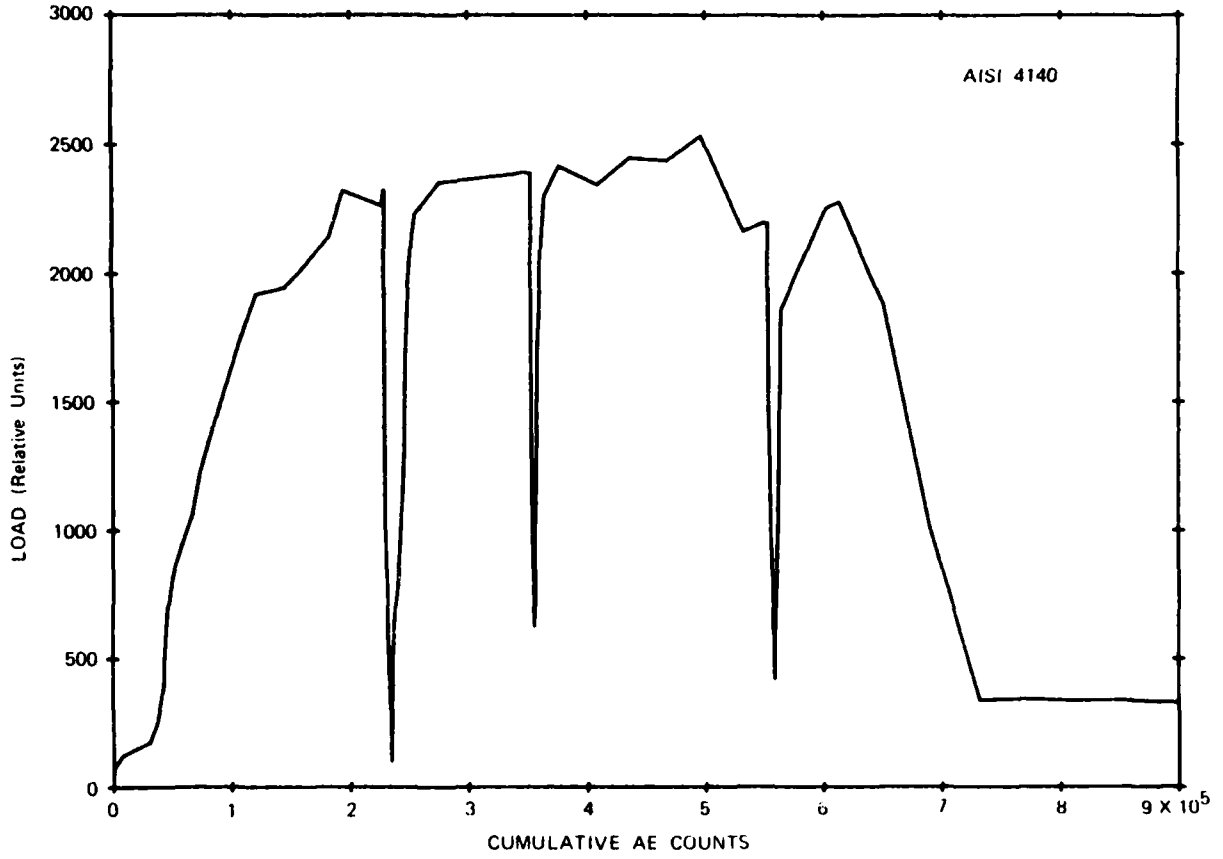

FIGURE 4 (b). Load versus cumulative AE counts for chevron-notched fracture toughness specimen, AISI 4140.

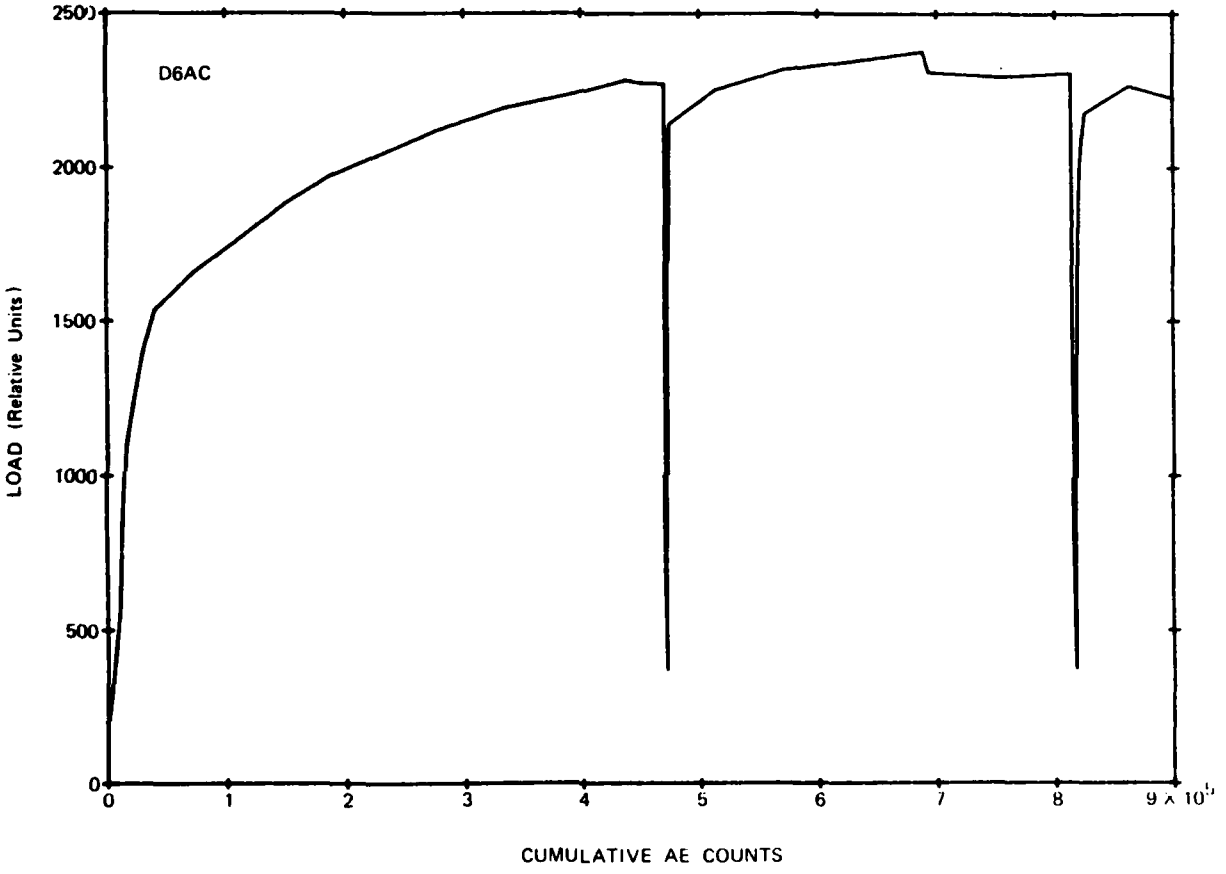

FIGURE 4 (c). Load versus cumulative AE counts for chevron-notched fracture toughness specimen, D6AC.

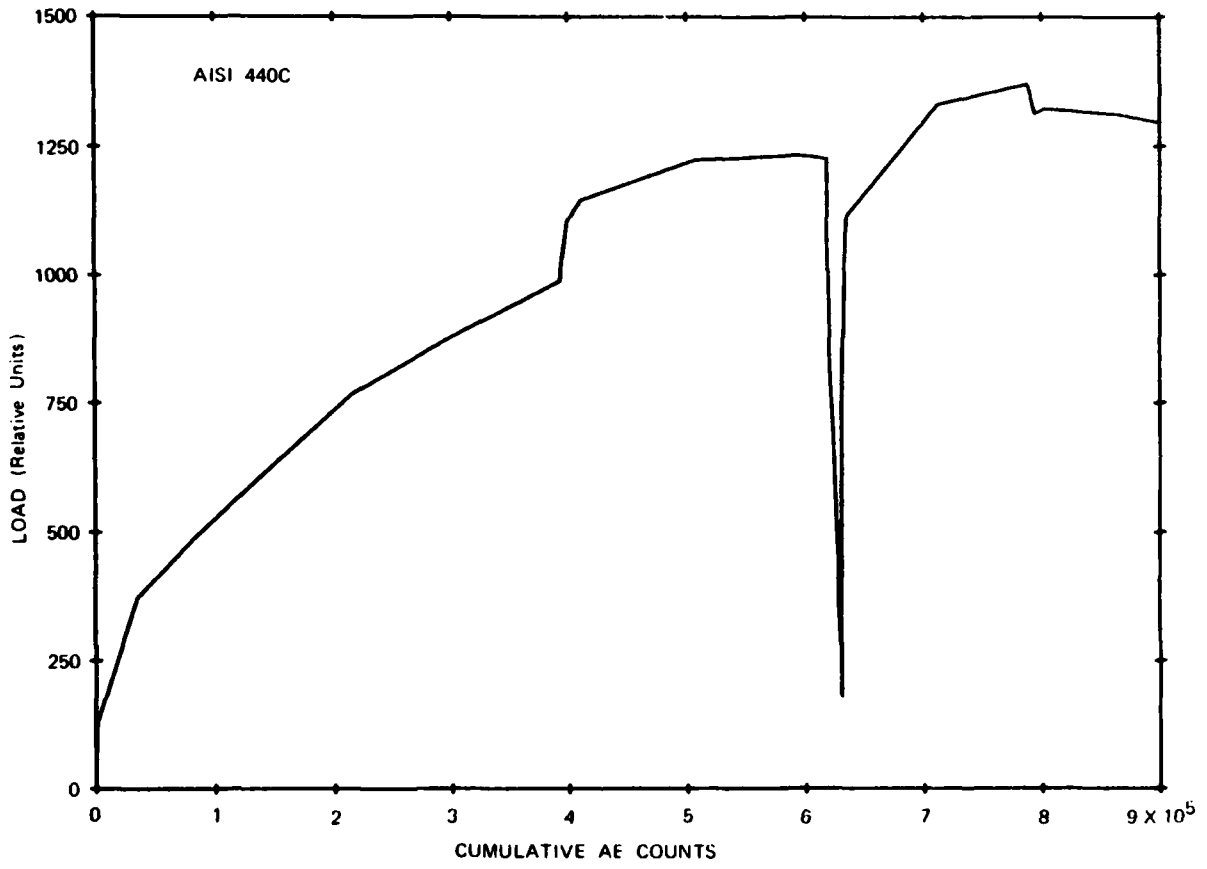

FIGURE 4 (d). Load versus cumulative AE counts for chevron-notched fracture toughness specimen, AISI 440C.

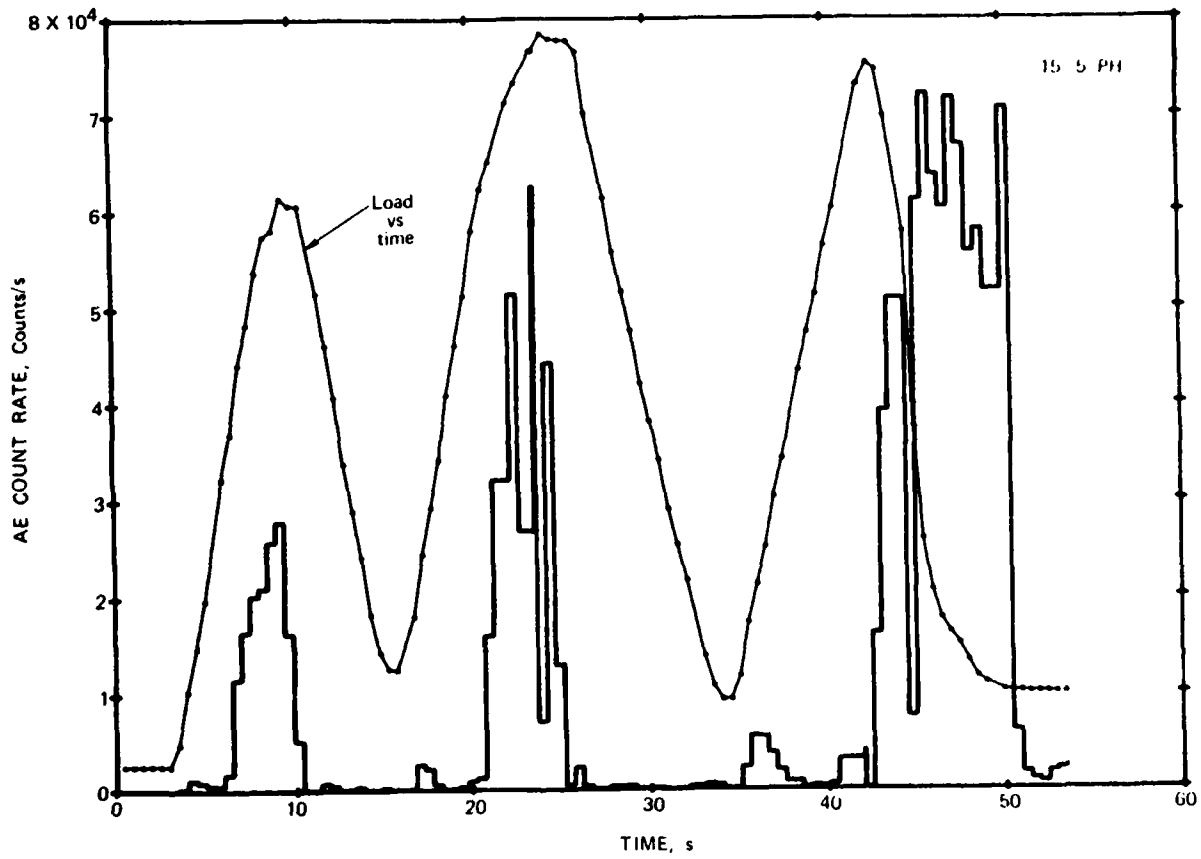

FIGURE 5 (a). AE count rate versus time for chevron-notched fracture toughness specimen, with plot of load versus time superimposed (dotted line), 15-5PH.

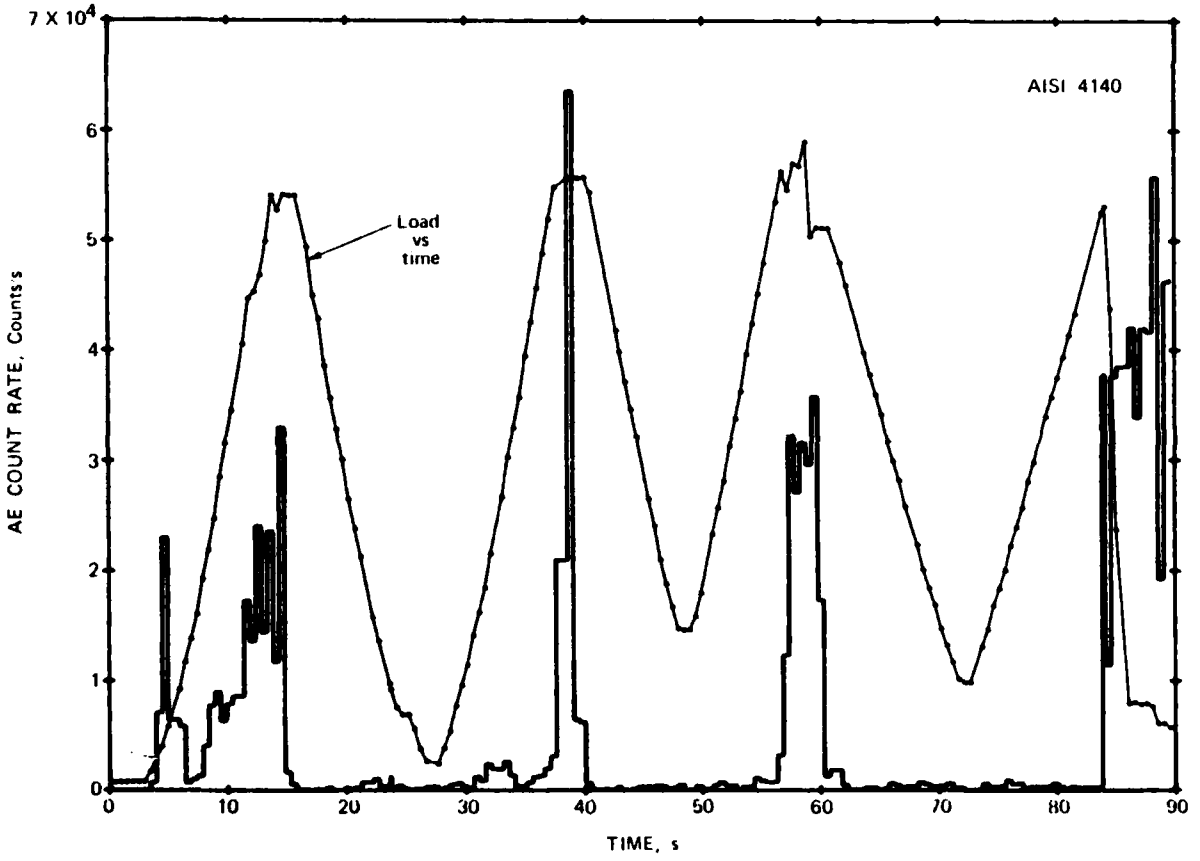

FIGURE 5 (b). AE count rate versus time for chevron-notched fracture toughness specimen, with plot of load versus time superimposed (dotted line), AISI 4140.

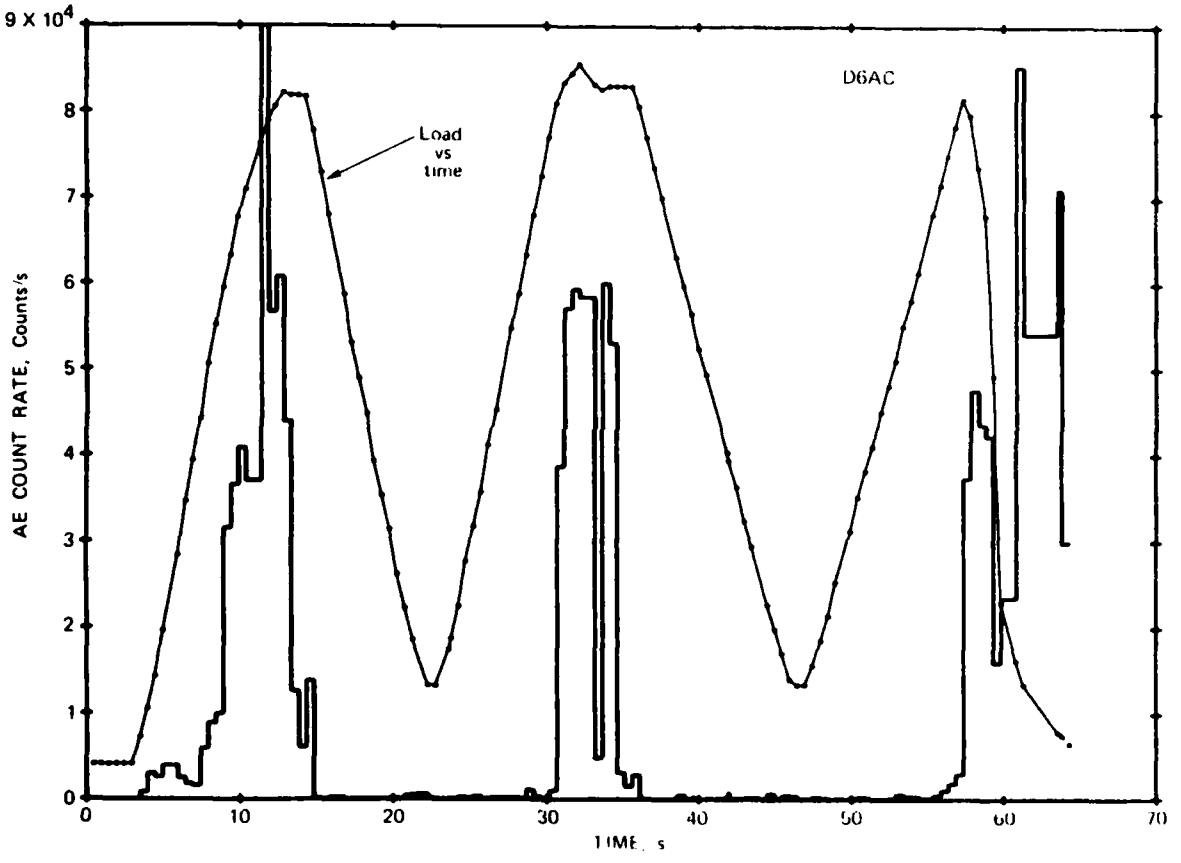

FIGURE 5 (c). AE count rate versus time for chevron-notched fracture toughness specimen, with plot of load versus time superimposed (dotted line), D6AC.

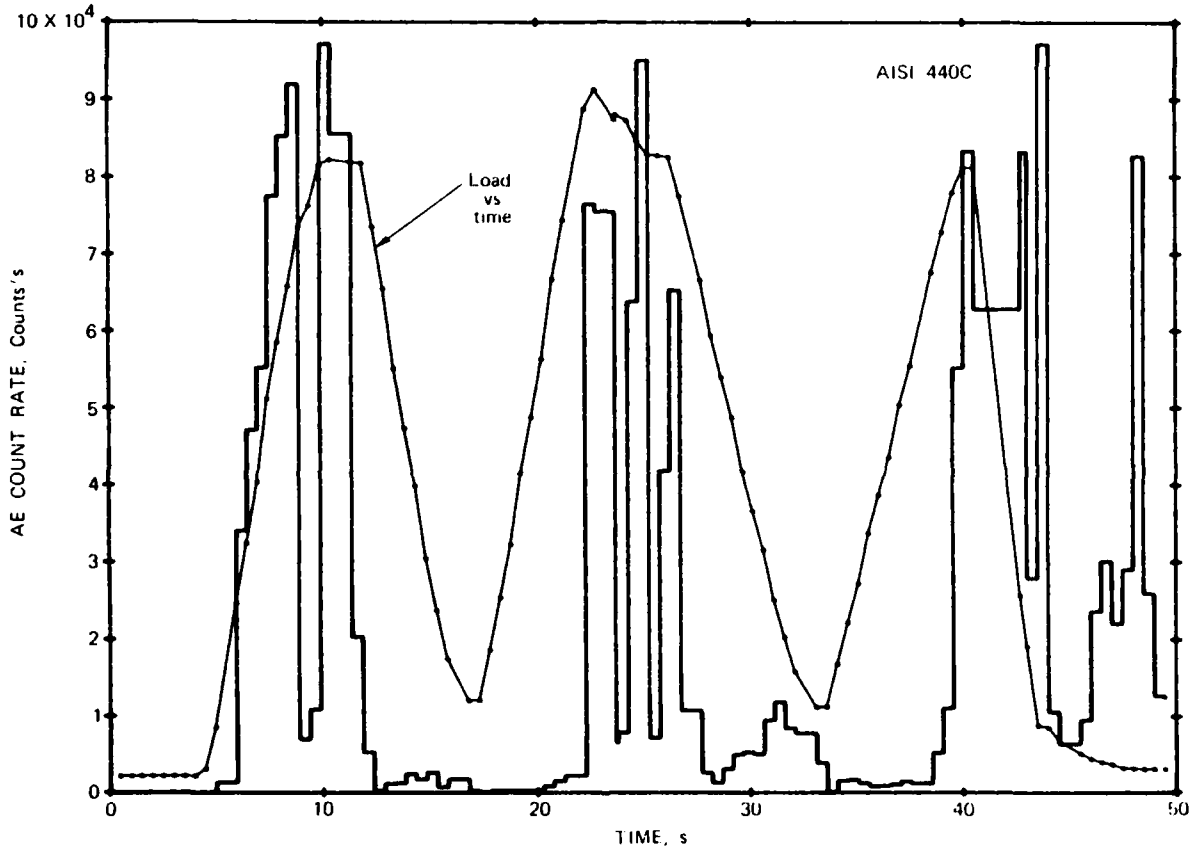

FIGURE 5 (d). AE count rate versus time for chevron-notched fracture toughness specimen, with plot of load versus time superimposed (dotted line), AISI 440C.

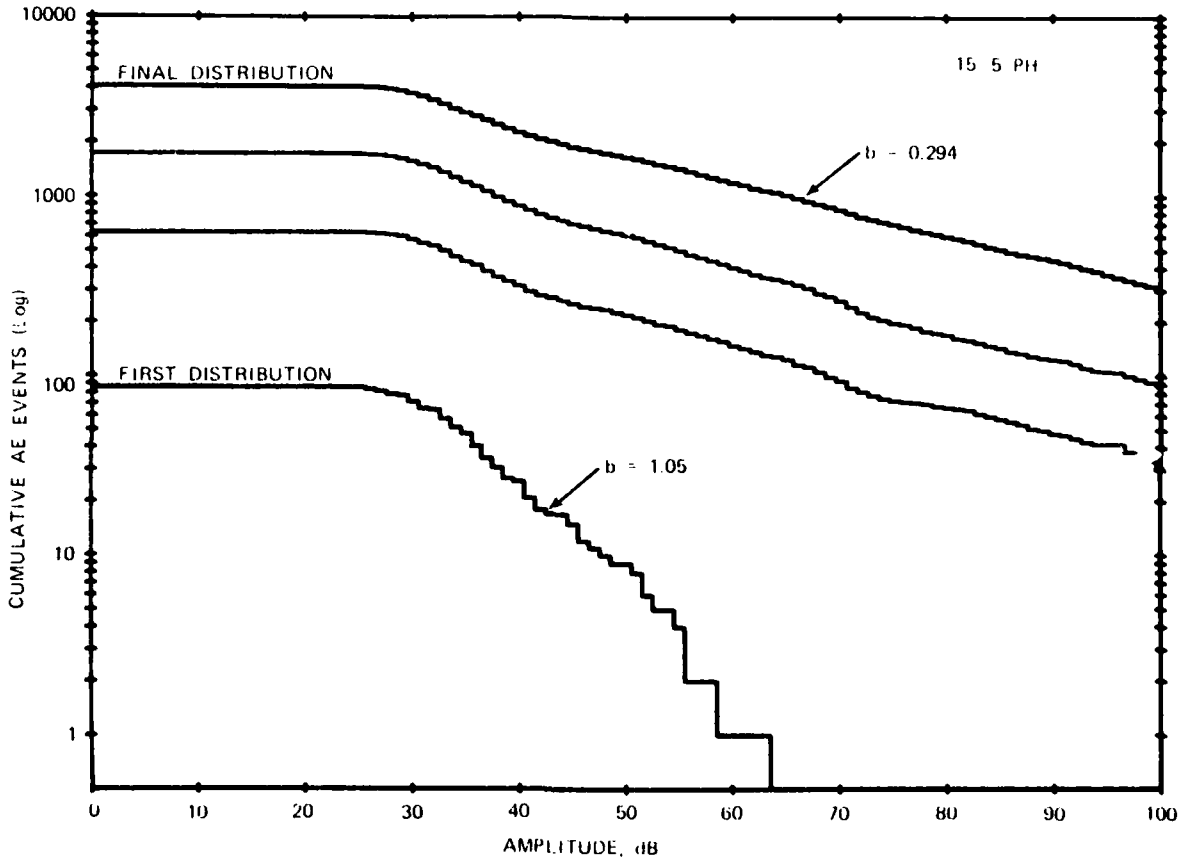

FIGURE 6 (a). AE amplitude distributions for chevron-notched fracture toughness specimen, 15-5PH. Threshold was set at 30dB.

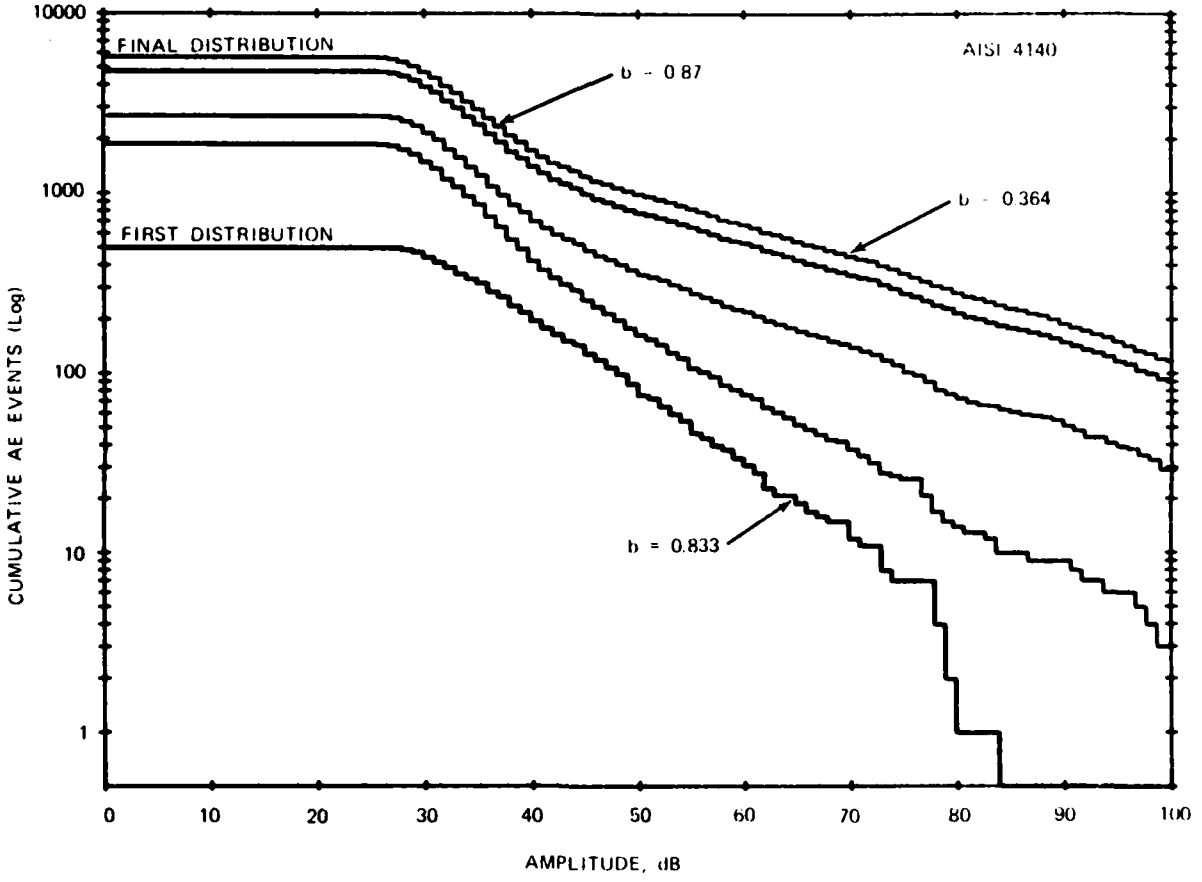

FIGURE 6 (b). AE amplitude distributions for chevron-notched fracture toughness specimen, AISI 4140. Threshold was set at 30dB.

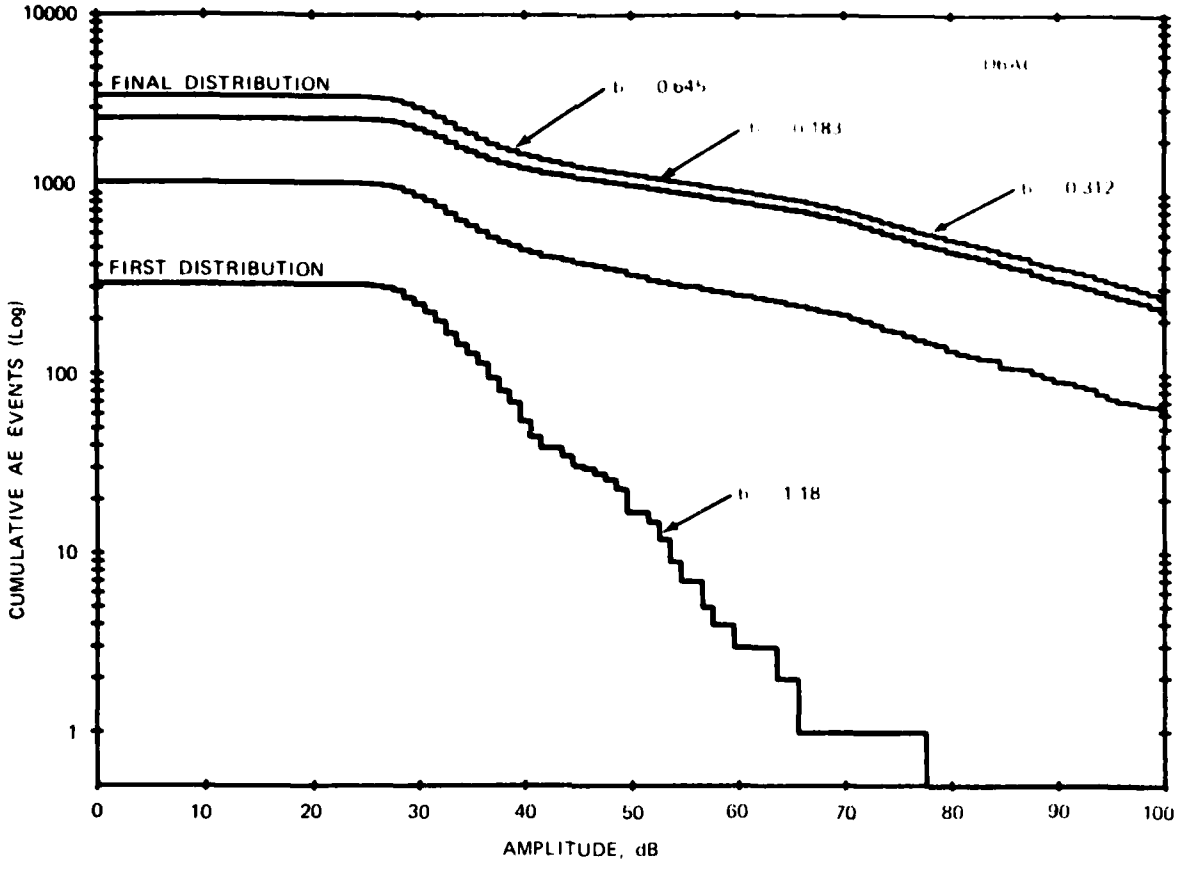

FIGURE 6 (c). AE amplitude distributions for chevron-notched fracture toughness specimen, D6AC. Threshold was set at 30dB.

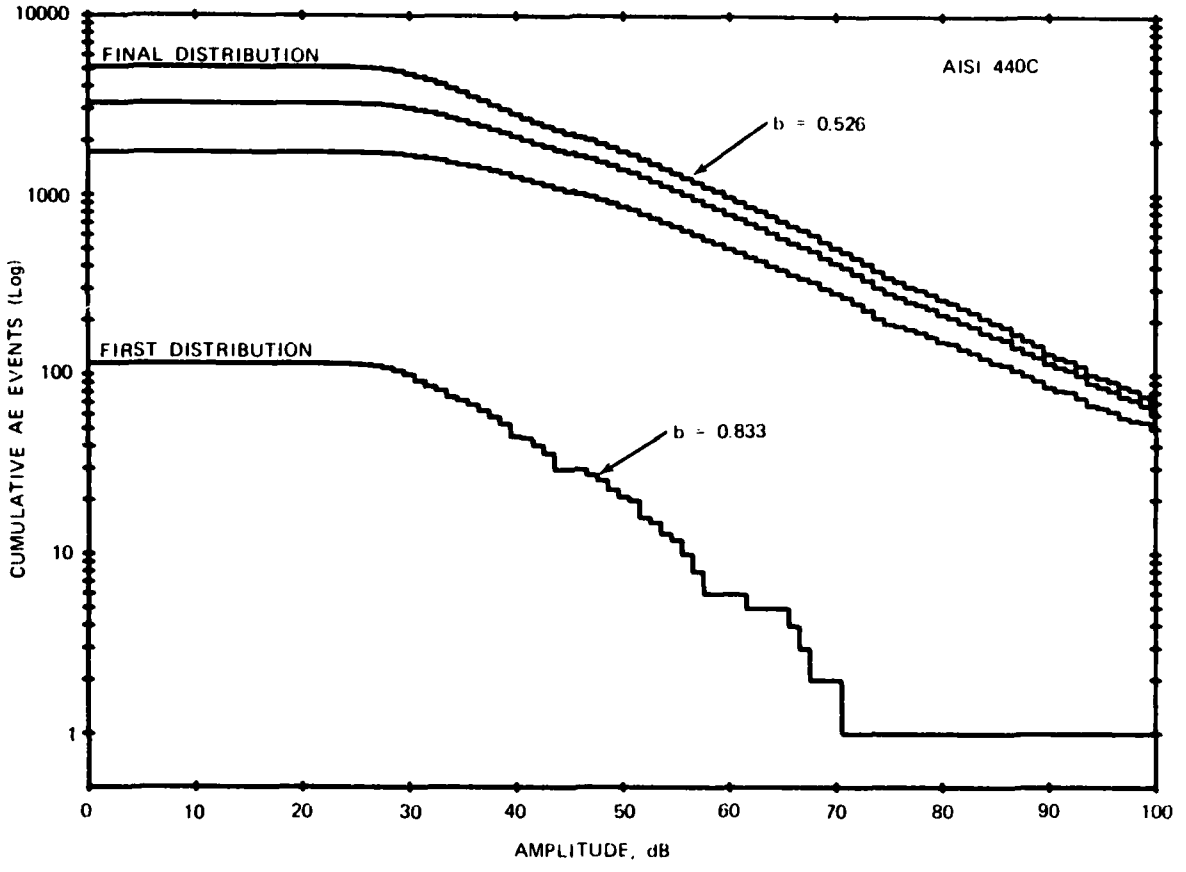

FIGURE 6 (d). AE amplitude distributions for chevron-notched fracture toughness specimen, AISI 440C. Threshold was set at 30dB.

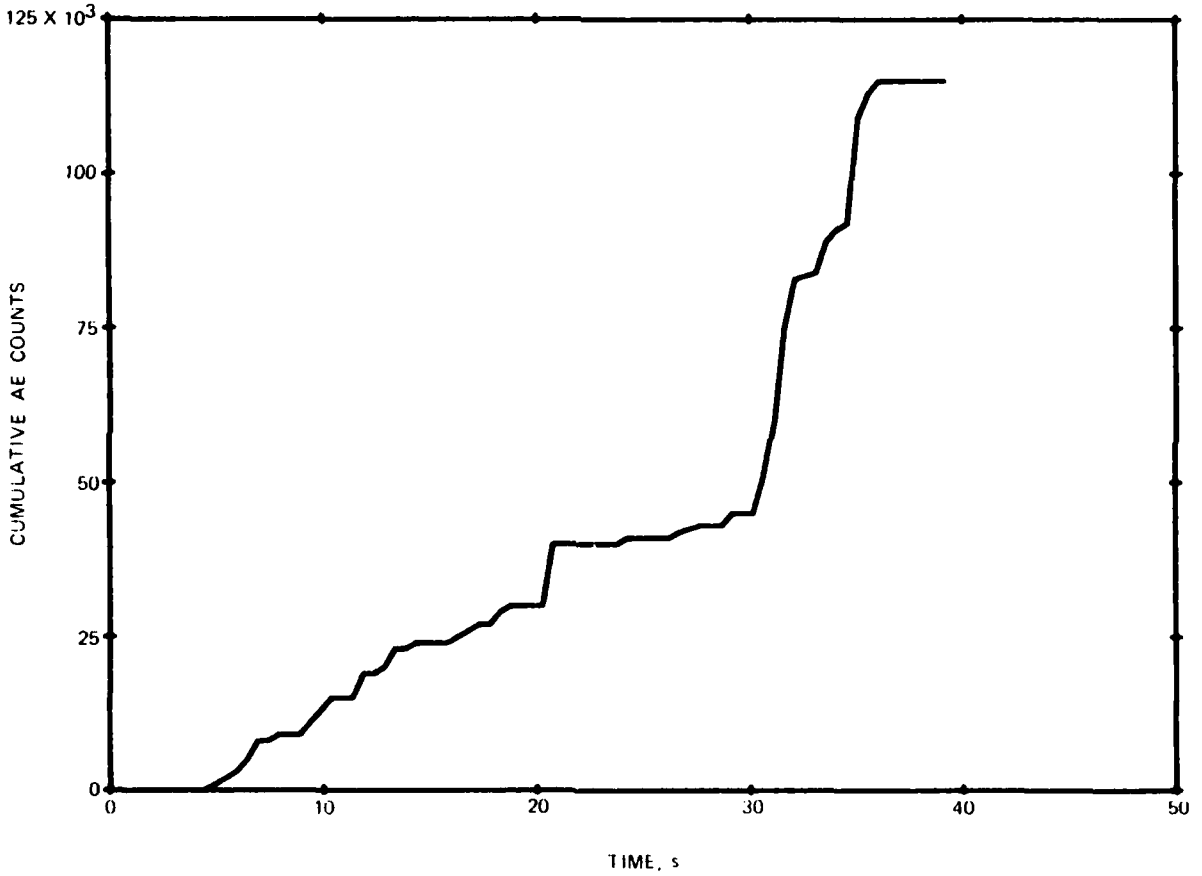

FIGURE 7 (a). AE versus time for loading and unloading of dummy specimen in TerraTak test fixture, AE cumulative counts. This test represents elastic deformation only.

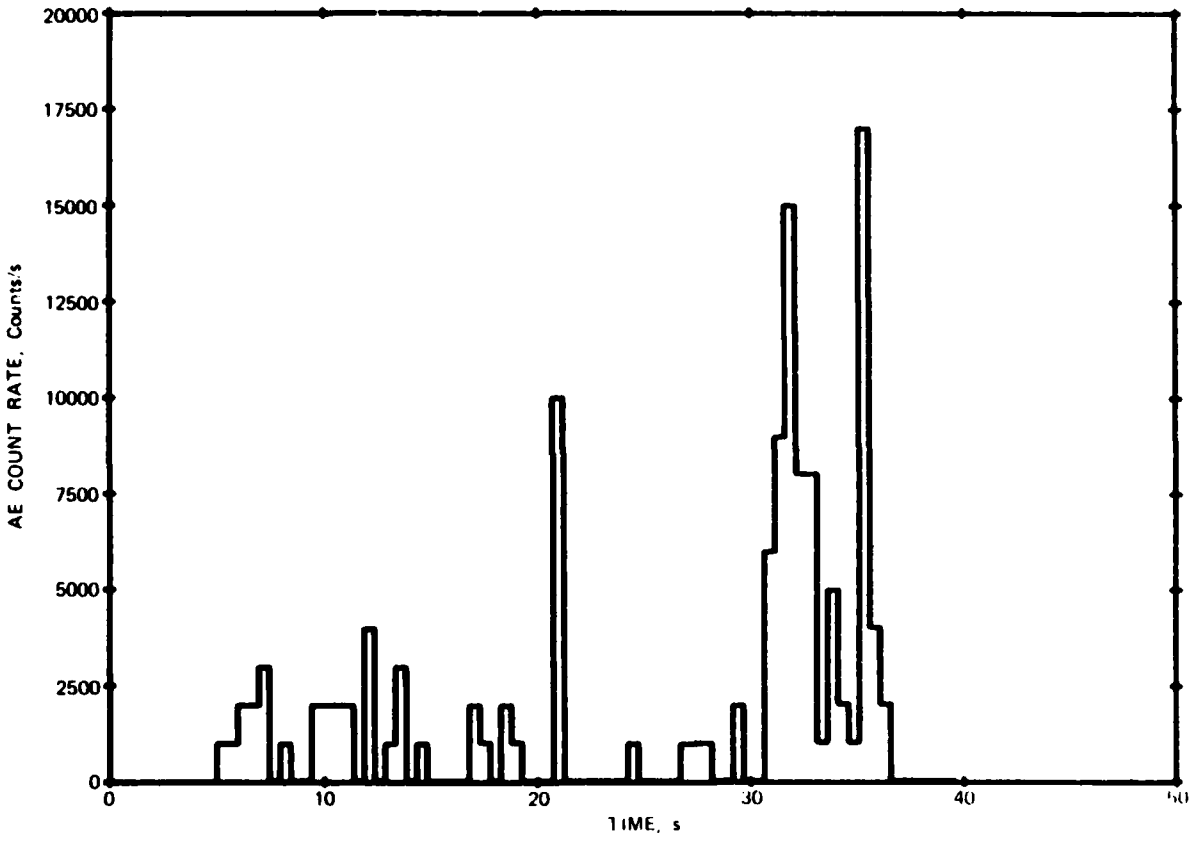

FIGURE 7 (b). AE versus time for loading and unloading of dummy specimen in TerraTek test fixture, AE count rate. This test represents elastic deformation only.

INITIAL DISTRIBUTION

11 Naval Air Systems Command
- AIR-00D4 (2)
- AIR-03D (1)
- AIR-301 (1)
- AIR-320 (1)
- AIR-5143 (1)
- AIR-516 (1)
- AIR-5302 (1)
- AIR-5304 (3)

2 Chief of Naval Research, Arlington
- ONR-461 (1)
- ONR-466 (1)

1 Naval Electronic Systems Command (ELEX-81341)

12 Naval Sea Systems Command
- SEA-05L (1)
- SEA-05M (1)
- SEA-05M1 (1)
- SEA-05M3 (1)
- SEA-05MT (1)
- SEA-05MX (1)
- SEA-05R25 (1)
- SEA-09B312 (2)
- SEA-62 (1)
- SEA-62C15 (1)
- SEA-62R4 (1)

1 Commander in Chief, U.S. Pacific Fleet (Code 325)

1 Commander, Third Fleet, Pearl Harbor

1 Commander, Seventh Fleet, San Francisco

1 Naval Academy, Annapolis (Engineering and Weapons Division)

1 Naval Air Test Center, Patuxent River (CT-252, Bldg. 405)

1 Naval Aviation Logistics Center, Naval Air Station, Patuxent River

1 Naval Ocean Systems Center, San Diego (Code 4472)

1 Naval Ordnance Station, Indian Head

1 Naval Postgraduate School, Monterey, (Department of Materials Science)

1 Naval Research Laboratory (Code 510)

3 Naval Ship Weapon Systems Engineering Station, Port Hueneme
- Code 5711, Repository (2)
- Code 5712 (1)

1 Naval Surface Weapons Center, White Oak Laboratory, Silver Spring (Technical Library)

1 Naval War College, Newport

1 Army Armament Research & Development Command, Dover (Technical Library)

3 Army Missile Command, Redstone Scientific Information Center, Redstone Arsenal (DRSMI-RPRD)

2 Army Ballistic Research Laboratory, Aberdeen Proving Ground
- DRDAR-TSB-S (STINFO) (1)

1 Harry Diamond Laboratories, Adelphi (Technical Library)

1 Rock Island Arsenal

2 Watertown Arsenal
- Director, Ordnance Materials Research Office (1)
- Technical Library (1)

1 Air University Library, Maxwell Air Force Base
1 Tactical Fighter Weapons Center, Nellis Air Force Base (COA)
2 57th Fighter Weapons Wing, Nellis Air Force Base
FWOA (1)
FWOT (1)
1 Defense Advanced Research Projects Agency, Arlington
12 Defense Technical Information Center
1 California Polytechnic State University, San Luis Obispo, CA (Department of Metallurgical Engineering)
1 Carnegie-Mellon University, Pittsburgh, PA (Department of Metallurgy)
1 Case Western Reserve University, Cleveland, OH (Department of Metallurgical Engineering)
1 Colorado School of Mines, Golden, CO (Department of Metallurgy)
1 Illinois Institute of Technology, Chicago, IL (Department of Metallurgical Engineering and Materials Science)
1 Iowa State University of Science and Technology, Ames, IA (Department of Metallurgical Engineering)
1 Massachusetts Institute of Technology, Cambridge, MA (Department of Materials Science and Engineering)
1 Montana College of Mineral Science and Technology, Butte, MT (Department of Metallurgy)
1 Northwestern University, Evanston, IL (Department of Metallurgical Engineering)
1 Ohio State University, Columbus, OH (Department of Metallurgy)
1 Pennsylvania State University, State College, PA (Department of Metallurgy and Materials Science)
1 Purdue University, West Lafayette, IN (Department of Metallurgical Engineering)
1 Stanford University, Stanford, CA (Department of Materials Science)
1 University of Arizona, Tucson, AZ (Department of Metallurgy)

1 University of California, Berkeley, CA (Department of Materials Science and Metallurgy)
1 University of California at Los Angeles, Los Angeles, CA (Department of Materials Science and Engineering)
1 University of Connecticut, Storrs, CT (Department of Metallurgical Engineering)
1 University of Florida, Gainsville, FL (Department of Metallurgical Engineering)
1 University of Idaho, Moscow, ID (Department of Metallurgical Engineering)
1 University of Illinois, Urbana, IL (Department of Metallurgy)
2 University of Utah, Salt Lake City, Ut
Department of Materials Science (1)
Department of Metallurgy (1)
1 University of Virginia, Charlottesville, VA (Department of Metallurgy and Materials Science)
1 University of Washington, Seattle, WA (Department of Metallurgy and Materials Science)
1 Washington State University, Pullman, WA (Department of Metallurgy and Materials Science)
1 Wayne State University, Detroit, MI (Department of Metallurgical Engineering)